

Unexpected large deformations in ^{60}Ni nuclei produced in the reaction $120\text{ MeV }^{30}\text{Si} + ^{30}\text{Si}$

G. La Rana, R. Moro, A. Brondi, P. Cuzzocrea, A. D'Onofrio, E. Perillo,
M. Romano, F. Terrasi, and E. Vardaci

*Dipartimento di Scienze Fisiche dell'Università and Istituto Nazionale di Fisica Nucleare,
Pad. 20 Mostra d'Oltremare, 80125 Napoli, Italy*

H. Dumont

*Service de Physique Nucléaire-Basse Energie, Centre d'Etudes Nucléaires de Saclay,
91191 Gif-sur-Yvette Cédex, France*

(Received 1 June 1987; revised manuscript received 22 January 1988)

Alpha energy spectra and angular distribution have been measured for the reaction $120\text{ MeV }^{30}\text{Si} + ^{30}\text{Si}$ and compared to statistical model calculations. Emission from spherical nuclei cannot account for the shapes of the measured spectra. Reductions are required in both emission barrier and entrance channel spin. A simulation of alpha evaporation from deformed nuclei has been carried out using an equivalent one-step code. Average values of mass, charge, spin, and excitation energy of the emitter were evaluated by a multistep evaporative code. The very large deformation required to reproduce the experimental data agrees with previous results which have suggested a need for new physics in statistical models.

I. INTRODUCTION

Evaporative light-charged particles have proved to be a powerful probe for the properties of the emitting nuclei such as temperature, effective emission barrier, and spin. A commonly used route to obtain such information is the comparison of the measured particle energy spectra and angular distribution with statistical model calculations. Recently, this kind of analysis was used to gain insight into the extent of the deformation of the emitting nuclei.¹⁻³ The rotating liquid-drop model (RLDM) (Ref. 4) predicts significant spin-induced deformations for highly rotating nuclei. Alexander, Guerreau, and Vaz¹ obtained equivalent spherical alpha emission barriers for a large set of emitting nuclei, analyzing mean energies and angular anisotropies for evaporative alpha spectra. They pointed out that differences between the deduced *s*-wave barriers and those for the reverse process (fusion of the alpha with the residual nucleus) are a strong indicator for a deformation of the emitter.

In order to investigate in detail these deformations, work has been done to include in the evaporative codes the effects of the emitter deformation on the particle spectra.⁵⁻⁷ These effects consist of (1) a lowering of the average effective emission barrier due to the deformation of the charge distribution and (2) an increase of the moment of inertia of the emitting nucleus. The first effect modifies the transmission coefficients for the evaporated particles, whereas the second one affects the level density of the residual nucleus.

In the reaction $214\text{ MeV }^{32}\text{S} + ^{27}\text{Al}$ (Ref. 8) the alpha particle spectra measured in coincidence with evaporation residues show deviations at both high- and low-energy side from the predictions of the statistical model for spherical nuclei. The data have been accounted for

by calculations which include large deformations in agreement with the prediction of the RLDM. Similar behavior has been found for the nucleus ^{67}Ga , produced in the reaction $190\text{ MeV }^{40}\text{Ar} + ^{27}\text{Al}$ (Ref. 2) at an excitation energy of 90 MeV and with a critical angular momentum for fusion $L_{\text{crit}} = 47\hbar$. The spectra and the angular distribution of evaporative alphas, compared with the statistical model for deformed nuclei,⁶ signal very strong deformations of the emitter ($b/a \geq 2$). On the other hand, the proton spectra cannot be reproduced even with this large deformation. This result has suggested that besides the deformation an additional source of distention of the nucleus must be invoked. Deformations for the same nucleus at higher angular momenta have been found in Ref. 7, using as a probe ^4He and ^1H spectra. A systematic study³ on several systems leading to compound nuclei with $23 \leq Z \leq 60$ with spins up to $60\hbar$ and temperatures $1.5\text{--}3.5\text{ MeV}$ indicates unexpected strong deformations for these emitters. Again proton spectra cannot be reproduced even with these large deformations.

In this paper we report on the study of evaporative ^4He emission in the reaction $120\text{ MeV }^{30}\text{Si} + ^{30}\text{Si}$ which produces the composite system ^{60}Ni at an excitation energy of 75 MeV and with a critical angular momentum of $38\hbar$, as derived from fusion cross-section data.^{9,10} We first present a comparison between measured ^4He energy spectra and the predictions of the statistical model for spherical nuclei using the code GANES.⁵ The equivalence between a multistep and an equivalent one-step calculation has been demonstrated using the code LILITA. Then we show the comparison between the data and the equivalent one-step code GANES which indicates deformations of the emitting nucleus ^{60}Ni . Finally, a comparison with statistical model calculations for deformed nuclei is presented.

II. EXPERIMENTAL PROCEDURE

The experiment was performed using a 120-MeV ³⁰Si beam provided by the XTU Tandem of the Laboratori Nazionali di Legnaro. The ⁴He energy spectra were measured in the singles mode using two- and three-stage Si telescopes, positioned at different angles with respect to the beam. They were calibrated by normalizing a pulser to the peak due to the 5.48-MeV ⁴He-particle decay of ²⁴¹Am. Ten angles have been measured in the range 35–150° corresponding to center of mass average angles of 55° to 165°. A thin layer of Au was evaporated on the target (about 150 μg/cm² of 95% isotopically enriched ³⁰Si), to obtain absolute cross sections by normalizing the data to the Rutherford elastic scattering of ³⁰Si on Au. The ratio between Au and Si thicknesses in the target has been measured by proton elastic scattering using the Tandem TTT-3 of the Dipartimento di Scienze Fisiche dell'Università di Napoli.

III. RESULTS AND DISCUSSION

In Fig. 1 a velocity contour map of the invariant ⁴He cross section is shown. The solid circular arcs are all centered on the tip of the center of mass velocity (as indicated by V_{c.m.} in Fig. 1). The agreement between the data and the circles indicates that pure evaporative emission from the compound nucleus dominates in the entire angular region. The relatively small deviations appearing at backward directions are attributable to angular anisotropies in the evaporative emission due to the spin of the emitting nucleus, as confirmed by the comparison between the measured energy spectra and statistical model calculations (discussed below). Similar deviations are expected at the symmetric forward angles in the center of

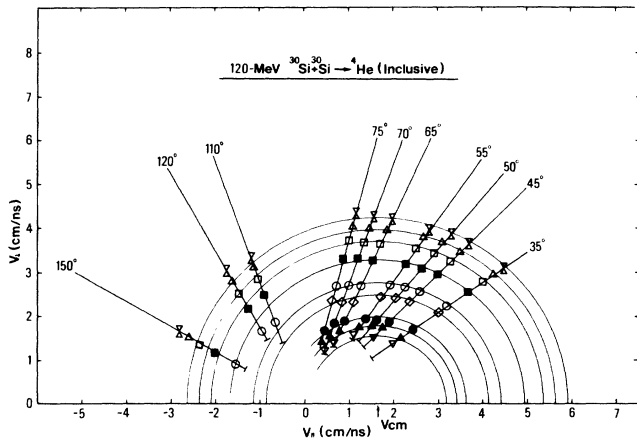


FIG. 1. Contour maps of the invariant cross section $(d\sigma/d\Omega dE)p^{-1}c^{-1}(\text{mb}/\text{sr MeV})$ for ⁴He emission. The axes V_{\parallel} and V_{\perp} denote laboratory velocity components parallel and perpendicular to the beam. The circular arcs are centered on the velocity of the center of mass $V_{c.m.}$. Detector thresholds are indicated on the straight lines drawn along the laboratory angles. The invariant cross-section magnitudes are: X, 1×10^{-6} ; \triangle , 1×10^{-5} ; \square , 1×10^{-4} ; \blacksquare , 1×10^{-3} ; \circ , 1×10^{-2} ; \diamond , 2×10^{-2} ; \blacklozenge , 1×10^{-1} ; \bullet , 2×10^{-2} ; \blacktriangle , 1×10^{-2} ; ∇ , 1×10^{-3} .

mass system, which correspond in the laboratory system to angles smaller than 35°. A significant amount of ⁴He preequilibrium emission, which for symmetric systems is expected with the same intensity at forward and backward directions, would produce deviations much stronger than those observed here.

A possible source of ⁴He particles is the emission from fragments of deep inelastic collisions (DIC), which has been identified for a similar system at the same incident energy.¹¹ We have simulated ⁴He evaporation from fragments of DIC using the center of mass total kinetic energy given in Ref. 12. The resulting energy spectra are much softer than the measured ones, as it can be seen in Fig. 2, where the comparison between the measured ⁴He energy spectrum at 35° and that simulated with the code GANES for projectilelike and targetlike fragments emission is shown. The calculated relative spectrum is normalized to the top of the experimental one for comparison. This supports the conclusion that the contribution to the experimental spectra of ⁴He particles coming from this process is negligible.

A. Comparison with the statistical theory for spherical nuclei

We show in Fig. 3 the measured energy spectra in the laboratory system (circles with occasional error bars).

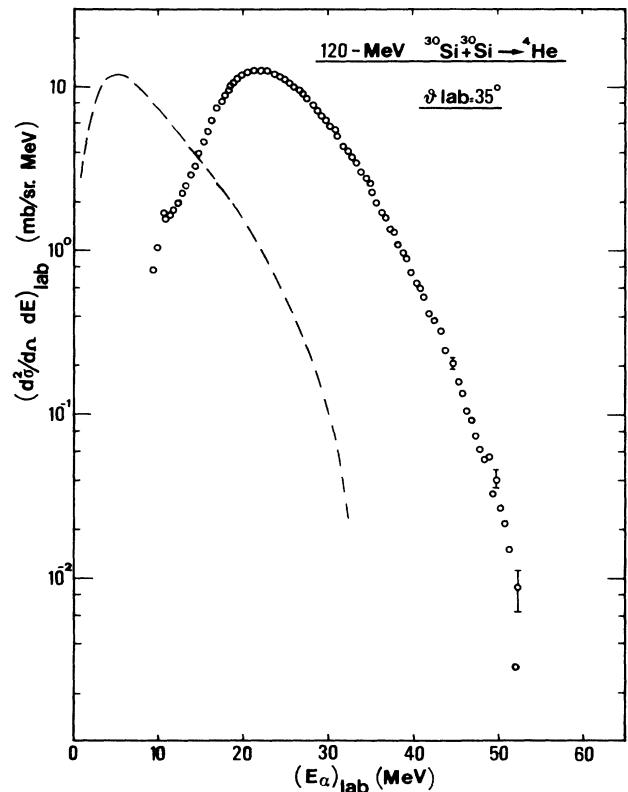


FIG. 2. Measured ⁴He energy spectrum ($\circ\circ\circ$) at 35° in the laboratory system compared with statistical model calculations for emission from projectilelike and targetlike fragments (---).

We first compare the data to a statistical model calculation for a spherical nucleus. Evaporation spectra have been obtained on the basis of the semiclassical statistical theory¹³⁻¹⁵ using the Monte Carlo code GANES. The program allows the simulation of the equivalent one-step emission of light particles from a spherical nucleus using an L -dependent transmission coefficient T_l (Ref. 16) and a spin-dependent Fermi gas level density.¹⁵ We have used a triangular spin distribution in the entrance channel characterized by $L_{\text{crit}} = 38\hbar$ and a fusion barrier for the reverse process from systematics¹⁷ ($B = 8.18$ MeV). The results of a calculation for a first-step emission are shown in Fig. 3 (dashed lines). The calculated relative spectra have been normalized to the measured spectrum at 55° in the laboratory system. As it can be seen, the calculation gives energy spectra shifted to higher energy with respect to the measured ones and significantly broadened. The behavior of this discrepancy suggests that the emitting nucleus is deformed. In fact, as already mentioned,^{6,15}

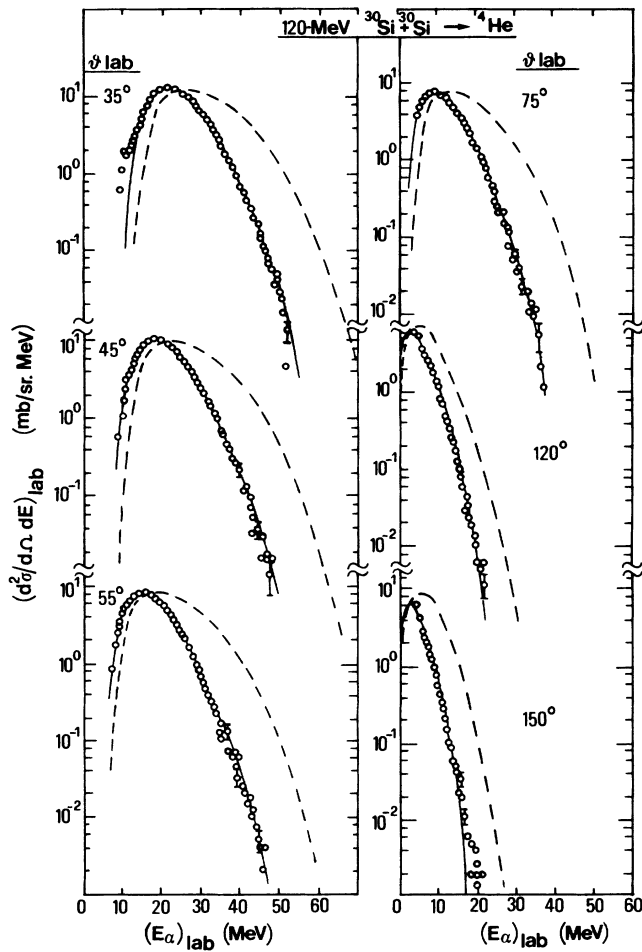


FIG. 3. Measured ${}^4\text{He}$ energy spectra ($\circ\circ\circ$) at different angles in the laboratory system compared with statistical model calculations for spherical nuclei: (---) using the fusion barrier $B = 8.2$ MeV and $L_{\text{crit}} = 38\hbar$; (—) using $B = 7.4$ and $L_{\text{crit}} = 26\hbar$. Results from calculations for deformed nuclei are almost undistinguishable from the solid lines.

nuclear deformations induce simultaneously a lowering of the effective emission barrier and an increase of the moment of inertia of the evaporating nucleus. The reduced barrier produces a shift to lower energy of the measured spectra. The larger moment of inertia produces a reduction of the width of the spectra and a decrease of the anisotropy, in case of not too heavy composite systems.

It must be pointed out that part of the found discrepancy could be ascribed to the first-step approximation used in the calculation. In fact, in a multistep calculation, which accounts for the entire evaporative chain, mean emission barrier, and spin, could be lower compared to the first-step values, if alpha particles are emitted in a wide range of excitation energy and spin in the evaporative chain. In order to gain insight on this point, we carried out a series of calculations with the multistep evaporative code LILITA,¹⁸ both in the first-step and the equivalent one-step modes. In particular, the aim was (a) to compare the results obtained assuming a first-step emission with those obtained assuming a multistep one, (b) to verify if the equivalent one-step calculation provides the same results (energy spectra and angular distribution) as a multistep one, when mean values of mass number A , charge Z , spin J , and excitation energy E_x of the emitter, deduced from the multistep calculation, are used. These parameters determine the barrier B , temperature T , and the anisotropy parameter β_2 , which in turn determine the shape of the energy spectra and the angular distribution.^{5,6} The points (a) and (b) are important as far as the use of codes based on a single-step emission are concerned, in particular for the code GANES which has been used here to calculate the emission from deformed nuclei.

In Fig. 4 we present the LILITA calculated energy spectra at $\theta_{\text{lab}} = 55^\circ$ and 110° together with the angular distribution in the center of mass system, assuming a first-step (—) and a multistep ($\circ\circ\circ$) emission. The spectra calculated as a first-step emission show a higher temperature resulting from the fact that the multistep calculation predicts that only 30% of the evaporated particles are emitted in the first step. At the same time the good agreement between the two calculated spectra at the low-energy side shows that “effects” on the emission barrier deriving from the multistep emission are negligible. Finally, the comparison between the angular distributions (bottom of Fig. 4) indicates that in our angular range the two calculations are equivalent. These conclusions can also be reached by looking at Table I (see row 2), where we report the mean values of A , Z , J , and E_x for the ${}^4\text{He}$ emitter calculated by the code LILITA, assuming a multistep calculation, together with the input parameters for the first-step calculation.

Concerning the point (b) mean values of A , Z , J , and E_x for the ${}^4\text{He}$ emitter deduced from the multistep calculation have been used in the equivalent one-step option in Lilita. The results of such a calculation are shown in Fig. 4 as dashed lines: the agreement with the multistep calculation is quite good. Similar agreement is found using different values of s -wave barrier and moment of inertia in the code LILITA. In particular, for the same values used in GANES ($B = 8.18$ MeV, $I = 11.35\hbar^2$ MeV $^{-1}$), the

agreement between a multistep and an equivalent one-step calculation is quite good, as shown in Fig. 5. The mean values of A , Z , J , and E_x deduced in this case, shown in Table I (see row 3), are slightly larger than those calculated previously, except for the excitation energy which is 10% larger. The increase in these parameters is related to the larger fraction of ^4He which are emitted in the first step (in this case 50%).

Although a detailed comparison between the codes GANES and LILITA is out of the aim of this paper, we have found that assuming a first-step emission in both programs, they are equivalent, provided that the same emission barrier and moment of inertia are used. To illustrate this point we show in Fig. 6 the energy spectra calculated at $\theta_{\text{lab}} = 52.5^\circ$ and 107.5° and the angular distribution calculated by GANES, compared with the prediction of LILITA in which we have introduced the emission barrier¹⁷ and moment of inertia of GANES. The agreement is good mainly because the level densities and the transmission coefficients used in the two codes are essentially equivalent. Both use a Fermi gas level density in the con-

TABLE I. Mean values of mass A , charge Z , spin J , and excitation energy E_x in MeV of the ^4He emitter in the deexcitation evaporative chain of the nucleus ^{60}Ni , obtained using the code LILITA. The input values for the first step are also reported.

	$\langle A \rangle$	$\langle Z \rangle$	$\langle E_x \rangle$	$\langle J \rangle$
First step	60	28	75.0	25.3
Multistep ^a	58.3	27.3	56.5	24.0
Multistep ^b	58.8	27.6	61.7	25.6

^aSee text.

^bSee text.

tinuum region,^{5,18} approximated by a constant-temperature level density. Concerning the transmission coefficients, LILITA uses a Fermi function which reproduces optical model transmission coefficients,¹⁸ while GANES uses the Hill-Wheeler expression¹⁶ with a curvature $\hbar\omega = 4.0$ MeV. Calculations show that the two transmission coefficients are essentially equivalent up to alpha particle energies of ≈ 20 MeV in center of mass. Differences appear at higher energies and arise from the different radius parametrization used by the two codes in the centrifugal barrier calculation and the L dependence

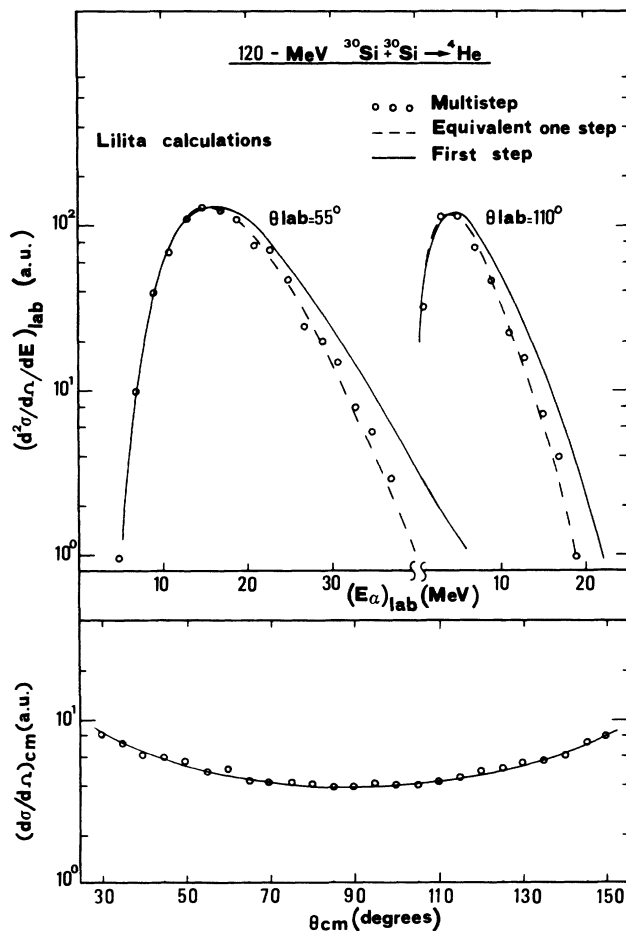


FIG. 4. ^4He energy spectra at $\theta_{\text{lab}} = 55^\circ$ and 110° and angular distributions calculated by means of the code LILITA, assuming a multistep emission ($\circ\circ\circ$), an equivalent emission ($---$) and a first-step emission ($-$). Average values of A , Z , J , and E_x of the emitter used in the second calculation are shown in Table I.

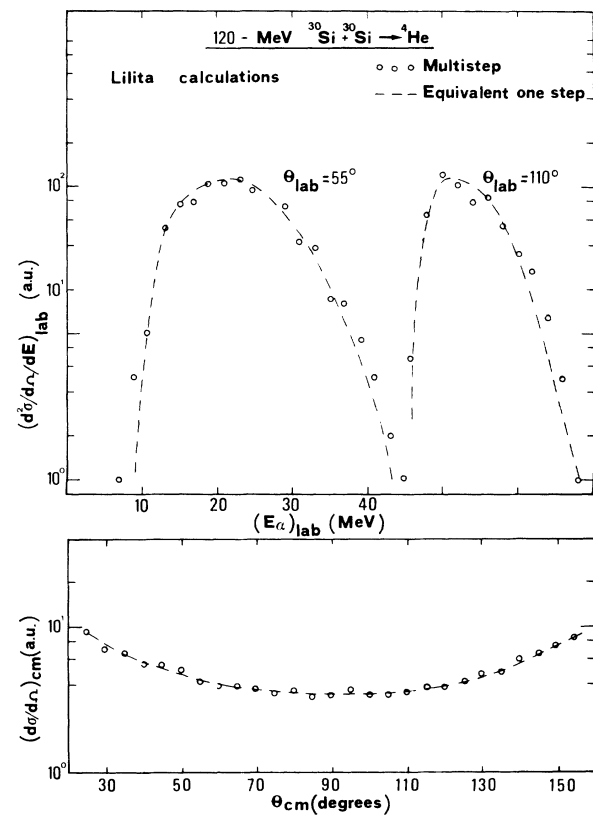


FIG. 5. ^4He energy spectra at $\theta_{\text{lab}} = 55^\circ$ and 110° and angular distributions calculated by means of the code LILITA assuming a multistep emission ($\circ\circ\circ$) and an equivalent one-step emission ($---$). The values of the emission barrier and moment of inertia used in the calculation are the same assumed by GANES.

of the barrier curvature in the Fermi function used in the code LILITA.

To simulate the deformation effects we have performed several calculations with the code GANES in the spherical option reducing the s -wave emission barrier and the maximum angular momentum characterizing the entrance channel spin distribution. The average values of A , E_x , and Z have been kept constant and equal to the values shown in Table I (see row 2). Data are well reproduced (solid lines in Fig. 3) using the values $B = 7.4$ MeV, $L_{\text{crit}} = 26\hbar$. Due to the strong constraints imposed by the measured spectra we can assign relatively small uncertainties to these (model-dependent) parameters. The good agreement at $\theta_{\text{lab}} = 150^\circ$ indicates that the deviations observed at backward directions in the invariant cross sections are essentially due to the spin-induced anisotropy.

The measured energy-integrated angular distribution is accounted for by both calculations shown in Fig. 3, as in the measured angular range the results are not very sensitive to different choices of the L_{crit} and barrier. In this respect measurements at more forward angles ($\theta_{\text{lab}} < 35^\circ$)

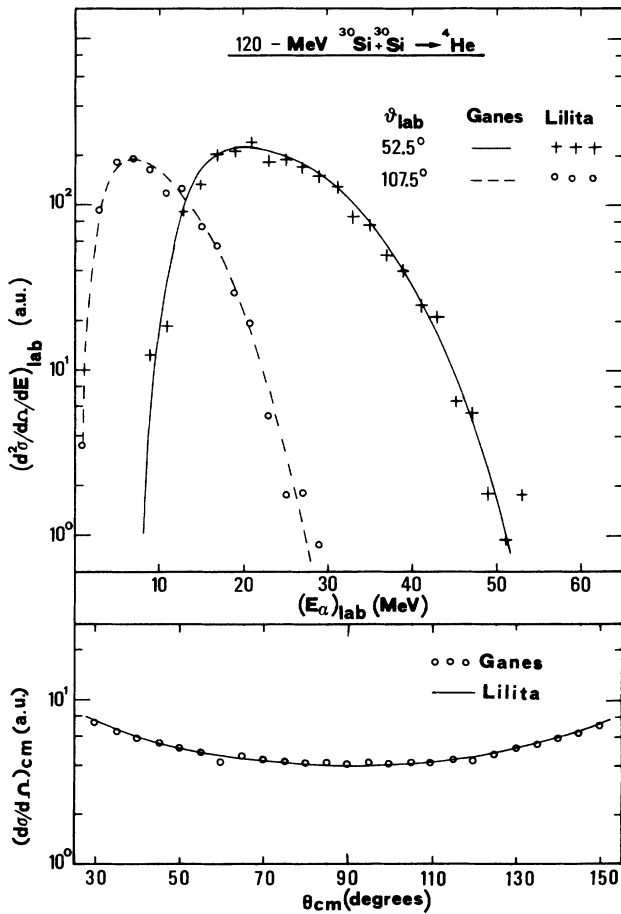


FIG. 6. ^4He energy spectra $\theta_{\text{lab}} = 52.5^\circ$ and 107.5° , and angular distributions calculated by the code GANES (—) and LILITA (---) assuming a first-step emission.

would provide strong constraints on the calculated angular distribution.

B. Comparison with the statistical model for deformed nuclei

Calculations for emission from deformed nuclei⁶ have been carried out using the code GANES. This option of the program allows to simulate the equivalent one-step emission of light particles from nuclei of different axially symmetric shapes: oblate, prolate, and pear shapes, besides the spherical one. A Cassinian system of orthogonal coordinates¹⁹ is used to describe the nuclear shapes. The effects of the charge distribution deformation on the emission barrier and of the increase of the moment of inertia on the centrifugal velocities of the evaporated particles are taken into account in the calculation. As far as the first effect is concerned, the barrier is calculated for different directions of the emitted particle with respect to the symmetry axis using a Wood Saxon nuclear potential for deformed nuclei proposed in Ref. 19. Its diffusivity is adjusted to reproduce for a spherical nucleus the barrier for the reverse process.¹⁷ The rotational energy, which appears in the level density, is calculated using the moment of inertia of the deformed nucleus. The L_{crit} value of $38\hbar$ was used to characterize the entrance channel L distribution. The shape of the emitter was the only free parameter, once the average values of A , Z , J , and E_x deduced from the spherical multistep calculation [Table I(a)] were provided. A good fit, almost indistinguishable from the full lines shown in Fig. 3, were obtained with an oblate shape with axis ratio ≈ 3.0 .

Concerning the deformation, the deduced very large axis ratio indicates that the simple deformation approach used here may be unrealistic. In fact, similar results have been found in Refs. 2 and 3, where the evaporative alpha spectra and the angular distribution measured for different systems demand for very strong deformations to be reproduced. On the other hand, the very low barriers observed in the proton spectra for these systems, could not be accounted for even with very large deformations. On these grounds it has been suggested^{2,3} that, besides the nuclear deformations, a new physics which effectively increases the mean evaporation radius, must be included in the statistical model. The results presented in this paper strongly support these conclusions.

IV. SUMMARY AND CONCLUSIONS

The ^4He energy spectra and angular distribution have been measured for the reaction $120 \text{ MeV } ^{30}\text{Si} + ^{30}\text{Si}$. The experimental spectra show emission barriers and widths significantly smaller than those predicted by the evaporation statistical model for spherical nuclei, indicating strong deformation of the emitting nucleus ^{60}Ni .

Calculations for ^4He emission from deformed nuclei have been carried out using the code GANES. Average values of A , Z , J , and E_x of the emitter deduced from the multistep code LILITA have been used in the equivalent one-step emission simulated by the code, leaving as free parameter only the shape of the nucleus. Data are well

reproduced assuming a very large oblate deformation ($b/a \simeq 3.0$). This unrealistic axis ratio indicates, as already suggested in Ref. 2, that additional physical effects, besides the deformation, must be taken into account to explain the particle emission from real nuclei.

ACKNOWLEDGMENT

The authors wish to thank Professor M. Kaplan and Professor J. M. Alexander for valuable discussions and suggestions.

-
- ¹J. M. Alexander, D. Guerreau, and L. C. Vaz, *Z. Phys. A* **305**, 313 (1982).
- ²G. La Rana, D. J. Moses, W. E. Parker, M. Kaplan, D. Logan, R. Lacey, J. M. Alexander, and R. J. Welberry, *Phys. Rev. C* **35**, 373 (1987).
- ³W. E. Parker, M. Kaplan, D. J. Moses, G. La Rana, D. Logan, R. Lacey, J. M. Alexander, D. M. de Castro Rizzo, P. DeYoung, and R. J. Welberry, report, 1988 (unpublished).
- ⁴S. Cohen, F. Plasil, and W. J. Swiatecki, *Ann. Phys. (NY)* **82**, 557 (1974).
- ⁵N. N. Ajitanand, R. Lacey, G. F. Peaslee, E. Duek, and J. M. Alexander, *Nucl. Instrum. Methods* **A243**, 111 (1986).
- ⁶N. N. Ajitanand, G. La Rana, R. Lacey, D. J. Moses, L. C. Vaz, G. F. Peaslee, D. M. de Castro Rizzo, M. Kaplan, and J. M. Alexander, *Phys. Rev. C* **34**, 877 (1986).
- ⁷Z. Majka, M. E. Brandan, D. Fabris, K. Hagel, A. Menchaca-Rocha, J. B. Natowitz, G. Nebbia, G. Prete, B. Sterling, and G. Viesti, *Phys. Rev. C* **35**, 21 (1987).
- ⁸R. K. Choudhury, P. L. Gonthier, K. Hagel, M. N. Namboodiri, J. B. Natowitz, L. Adler, S. Simon, S. Kniffen, and G. Berkowitz, *Phys. Lett.* **143B**, 74 (1984).
- ⁹H. Dumont, B. Delaunay, D. M. Rizzo, A. Brondi, P. Cuzzocrea, A. D'Onofrio, R. Moro, M. Romano, and F. Terrasi, *Nucl. Phys.* **A435**, 301 (1985).
- ¹⁰Y. Nagashima, J. Schimizu, Y. Fukuchi, W. Yokota, K. Furuno, M. Yamanouchi, S. M. Lee, N. X. Dai, and T. Mikumo, *Phys. Rev. C* **33**, 176 (1986).
- ¹¹C. Manduchi, M. T. Russo Manduchi, G. F. Segato, and F. Andolfato, *Nuovo Cimento* **96A**, 213 (1986).
- ¹²V. E. Viola, K. Kwiatkowski, and M. Walker, *Phys. Rev. C* **31**, 1550 (1985).
- ¹³T. Ericson and V. Strutinski, *Nucl. Phys.* **8**, 284 (1958); **9**, 689 (1959).
- ¹⁴T. Ericson, *Adv. Phys.* **9**, 425 (1960).
- ¹⁵T. Dossing, Licentiat thesis, University of Copenhagen, 1977.
- ¹⁶D. L. Hill and J. A. Wheeler, *Phys. Rev.* **89**, 1102 (1953).
- ¹⁷L. C. Vaz and J. M. Alexander, *Z. Phys. A* **318**, 231 (1984).
- ¹⁸J. Gomez del Campo and R. G. Stokstad, Oak Ridge National Laboratory Report No. TM7295, 1981 (unpublished).
- ¹⁹V. V. Pashkevich, *Nucl. Phys.* **A169**, 275 (1971).